NDE2002 predict. assure. improve.
National Seminar of ISNT
Chennai, 5. – 7. 12. 2002
www.nde2002.org

Measurement of phase velocity dispersion curves and group velocities in a plate using leaky Lamb waves

Young H. Kim[1], Sung-Jin Song[1], and Sung-Duk Kwon[2]

[1]School of Mechanical Engineering, Sungkyunkwan University, Suwon, 440-746 Korea
[2]Department of Physics, Andong National University, Andong, 760-749 Korea

ABSTRACT. The guided wave has been widely employed to characterize thin plates and layered media. The dispersion curves of phase and group velocities are essential for the quantitative application of guided waves. The technique using leaky Lamb wave (LLW) is one of the excellent methods to obtain dispersion curves. In the present work, a fully automated system for the measurement of LLW has been developed. The specimen moves in two dimensional plane as well as in angular rotation. The signals of LLW were measured from an elastic plate in which specific modes of Lamb wave were strongly generated. Phase velocity of the corresponding modes was determined from the incident angle. The generated Lamb waves propagated along the plate, were reflected at the edge of the plate. A portion of Lamb wave was leaked into water, so that it was detected by the same transducer. Frequency components of the detected signals were analyzed to extract the related information to the dispersion curves. The dispersion curves of phase velocity were measured by varying the incident angle. Moving the specimen in the linear direction of LLW propagation, group velocity was determined by measuring the transit time shift in the rf waveform.

INTRODUCTION

Ultrasound has been widely used for the materials characterization as well as flaw detection. Ultrasonic methods usually measure the transient time and amplitude, so that they require enough distances for beam propagation. Therefore, it is difficult to evaluate thin plates using conventional ultrasonic methods. It has been well known for a long time that guided waves are suitable to evaluate a thin plate than the conventional bulk waves [1-3]. Lamb waves are guided waves propagating in a plate. Another advantage of ultrasonic testing with guided waves is the capability of long range inspections [4]. In ultrasonic guided waves, however, there are numerous modes. Wave velocity varies not only by the elastic properties and density of the medium, but also by frequency, the thickness of plate and wave mode, which is known as the dispersion. At a given frequency and plate thickness, several modes may propagate with different velocities. At a given phase velocity, several modes can be excited with different frequencies. And the group velocity which is the propagation speed of wave energy is different from the phase velocity. Therefore, the dispersion characteristics of a plate should be understood thoroughly for the appropriate application of guided waves. Another importance of dispersion curves of phase velocity is that the mechanical properties and the thickness of a plate could be determined from the dispersion curves [5].

In order to measure velocities of Lamb waves, the transit time has to be measured using two transducers in the pitch-catch setups or using one transducer in the pulse-echo setups that catches the reflection from the edge of the plate. However, obtained ultrasonic signal is distorted by the dispersion of Lamb wave and it is hard to determine the wave mode and transit time precisely. In addition to this difficulty, measured velocity is not the phase velocity but the group velocity. A numerous works to determine dispersion curves of phase velocity have been carried out. For example, the line focused PVDF transducer [6] and the laser generated ultrasound [7,8] were employed for this purpose.

In the case of immersion techniques, the Lamb waves "leak" out from the plate as they propagate, so that they are termed "leaky" Lamb waves. The LLW wave technique uses specific modes of the guided wave which is generated and detected through the mode-converted waves in the medium surrounding the plate. Some energy of Lamb wave can be caught by a single transducer in a pulse-echo setup.

In the present work, an automatic system for the measurement of leak Lamb wave was constructed in order to obtain the phase velocity dispersion curves. The LLW wave which had been reflected at the edge of specimen was captured by varying the incident angle. The dispersion curves of phase velocities were determined from the relation between incident angles and the frequency spectra of LLW. The group velocities were determined from the time delay caused by moving the incident position

LEAKY LAMB WAVES

Fig. 1 shows the schematic diagram of LLW generation. Let us consider ultrasound that is incident on a plate in water. The ultrasound incident at a certain angle will be reflected without distortion if there is no phase matching between the incident wave and one of the Lamb wave modes. On the other hand, when the phase matching takes place, the Lamb wave is generated, propagates along the plate and is reflected at the edge of the plate. Some energy of them leaks into water and produces reflected and transmitted beam. Reflection at the edge of the plate can be caught by a single transducer in a pulse-echo setup [9,10].

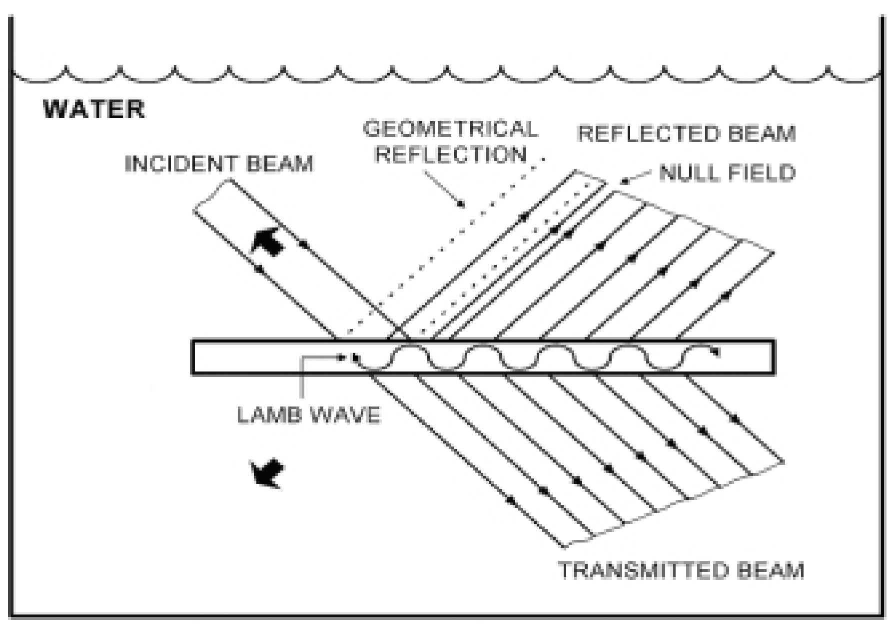

FIGURE 1. Schematic diagram of leaky Lamb wave generation [1].

The condition for the phase matching is satisfying the Snell's law, which is given as:

$$\frac{c_i}{\sin\theta_i} = \frac{c_r}{\sin\theta_r} \tag{1}$$

where, c_i and c_r are velocities of incident and refracted waves, respectively, and θ_i and θ_r are the incident and refracted angles, respectively.

When Lamb waves propagate along the plate, the velocity of incident wave is equal to the wave speed in water, c_f, velocity of refracted wave is the phase velocity of Lamb wave, c_p, and refraction angle is 90°. Thus, Eq. (1) becomes

$$c_p = \frac{c_f}{\sin\theta_i}\ . \tag{2}$$

Eq. (2) implies that the phase velocity of Lamb wave generated in a plate can be determined from the incident angle.

EXPERIEMENTAL SETUP

Figure 2 shows the system developed for the measurement of LLW. The specimen used in the present work was maraging steel with the thickness of 0.64 mm. The specimen was rotated to change incident angle and translated in horizontal and vertical direction to change the incident position. All motions were driven by three computer controlled microstep motors. Accuracies in rotation and translation were 0.02° and 20 micrometer, respectively.

The transducer of 5MHz broadband type and a Panametrics 5800 ultrasonic pulser-receiver were employed to generate and receive ultrasonic waves. Backward radiated ultrasound was captured and digitized by a Lecroy LT342 digital oscilloscope. Motion control and ultra sonic data acquisition were fully automated.

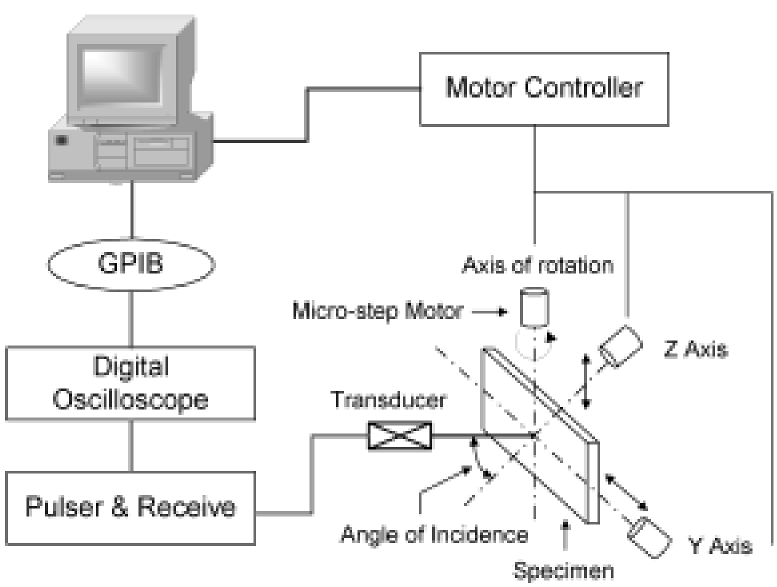

FIGURE 2. Schematic diagram of experimental setup of LLW measurement.

RESULTS AND DISCUSSION

Mode Analysis of Backward Radiated Ultrasound

The LLW from a steel plate was measured with varying the incident angle. LLW were observed for all of incident angles. Figure 3 shows the profile of LLW, which is angular variation of backward radiated ultrasound amplitude. Three major peaks were clearly observed in this profile at the incident angles of 14.3º, 16.0º and 30.0º. The peak at 30.0 degree was also observed in the profiles of a bulk specimen, corresponding to the Rayleigh surface wave. However, the other peaks were not able to be observed in the profile of the bulk specimen.

Figure 4 and 5 show typical rf waveforms and frequency spectra of LLW from the plate at the incident angles of 14.3º and 16.0º, respectively. Even with the small amount of change in the incident angle (about 1.7º), the waveform of LLW varied significantly in their shapes as well as amplitudes. Especially, two distinct wave packets with different frequencies were clearly observed in the rf waveform in Figure 5. Since the transit times of two wave packets are different, the group velocities of two wave packets are, of course, different. Thus, the two wave packets different wave modes.

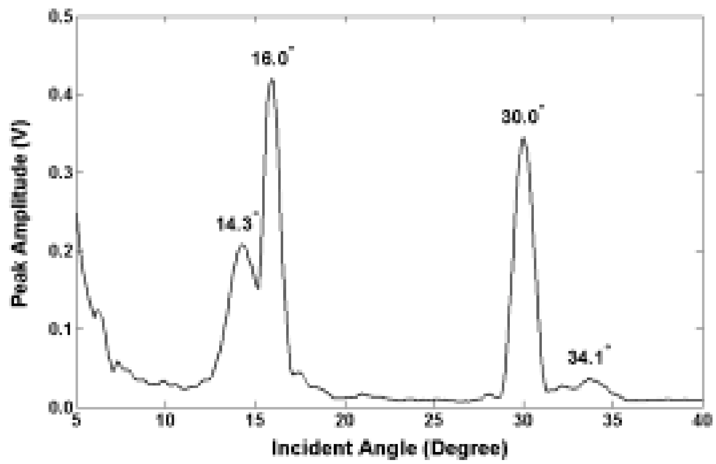

FIGURE 3. Angular dependence of LLW amplitude.

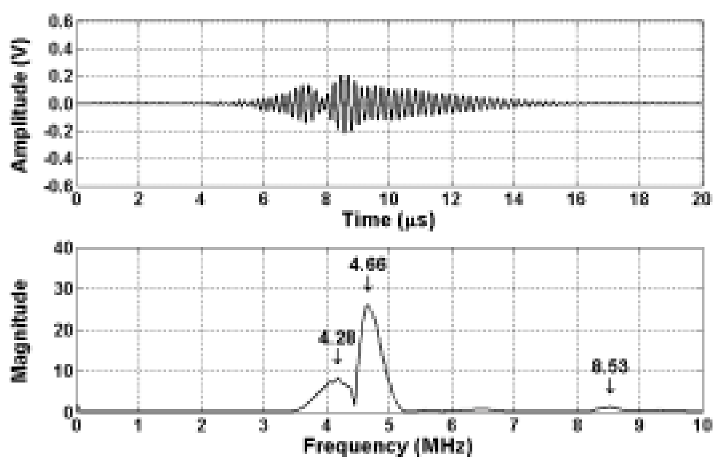

FIGURE 4. The rf waveforms and frequency spectrum of the LLW at the indent angle 14.3º.

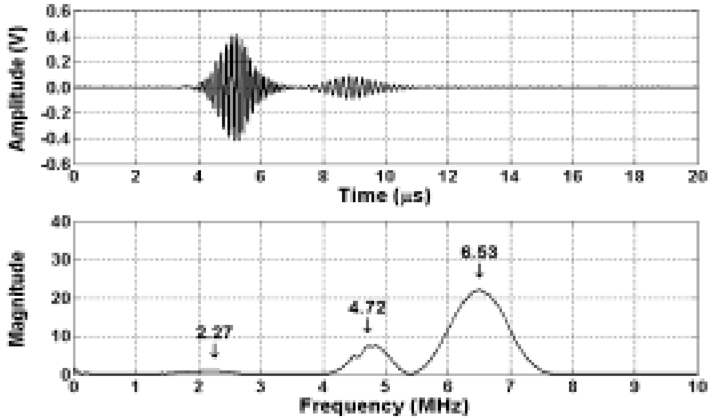

FIGURE 5. The rf waveforms and frequency spectrum of the LLW at the indent angle 16.0º.

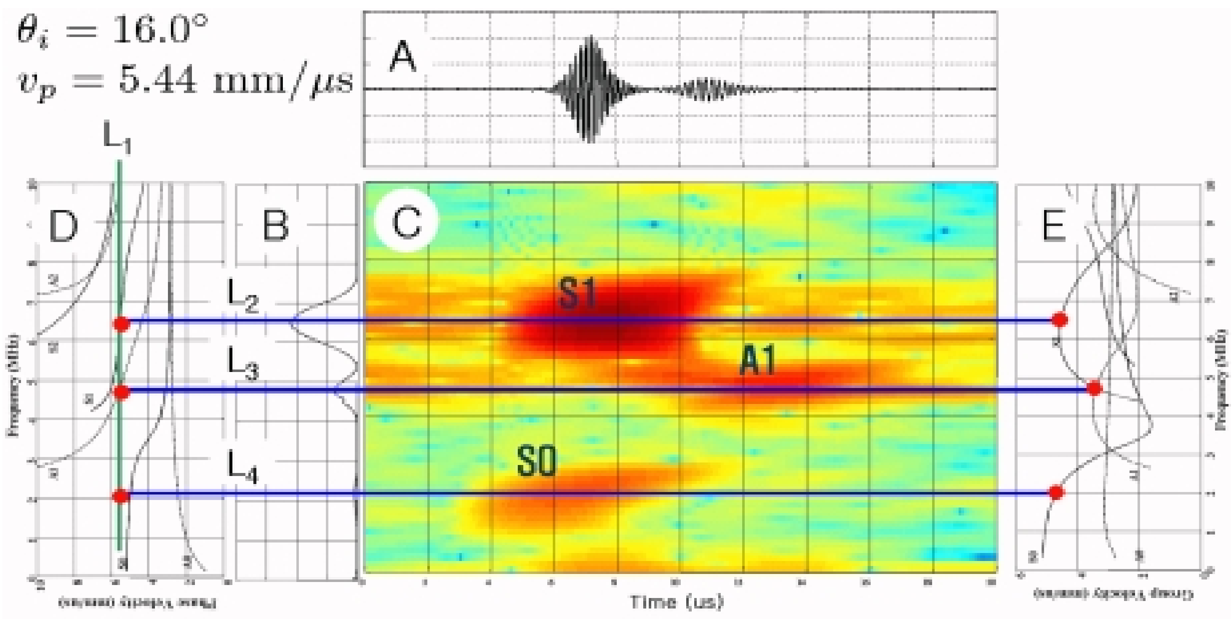

Figure 6. Relationship among Time domain waveform (A), frequency spectrum (B), time-frequency analysis (C), dispersion curves of phase (D) and group (E) velocities.

Two distinct wave packets in the time domain waveform and three peaks in the frequency spectrum were observed in Figure 5. Since the incident angle was 16º, the phase velocity of Lamb wave modes in the plate was 5,440 m/s from the Eq. (2). The frequencies of the matched Lamb wave modes were 2.27, 4.72, 6.53 MHz from the frequency spectrum shown in Figure 5. Time-frequency analysis such as the short time Fourier transform (STFT) as shown in Figure 6 gives much more information to the LLW modes.

Figure 6 shows detail procedures of the signal analysis used in the present work. ‘A’ and ‘B’ are waveform and frequency spectrum of backward radiation, respectively, as similar to Figure 5. ‘C’ shows the STFT of the time domain waveform of backward radiation. ‘D’ and ‘E’ are calculated phase and group velocity dispersion curves, respectively. A vertical line, ‘L_1’ indicates the phase velocity value determined by the incident angle, and the three horizontal lines, ‘L_2’, ‘L_3’ and ‘L_4’ indicate the peak frequencies obtained from the frequency spectrum, ‘B’. Three dots at which the vertical and horizontal lines crosses indicate phase matching conditions, and they are on the phase velocity dispersion curves of S_1, A_1 and S_0 modes. Therefore, peak frequencies of 2.27,4.72 and 6.53 MHz in Figure 5 are corresponding to S_0, A_1 and S_1 modes of Lamb wave.

The STFT shows also three distinct modes. The first arrived mode of small amplitude and lowest frequency in STFT, which is hard to be figured out in time domain waveform, is identified as S_0 modes from the dot closing 'L_1' and 'L_4'. Other modes were also identified as similar manner. The group velocities were also determined from the dots at which horizontal lines and the group velocity dispersion curves of corresponding modes cross. The group velocities determined by this manner showed a good agreement with the fact that the mode with faster group velocity arrived earlier. Therefore, the modes of the backward radiation were successfully identified and the corresponding phase velocities were determined accurately. It has been figured out by the same procedure that the peak frequencies of 4.28,4.66 and 8.53 MHz in Figure 4 were corresponding to A_1, S_1 and S_2 modes of Lamb wave.

Dispersion Curves of Phase Velocity

As mentioned in the previous section, we were able to obtain the information related to the dispersion curves from the LLW. The LLWs were captured with varying the incident angles from 5° to 45° in the step of 0.1°. The frequency spectra of captured signals were represented in gray scale, and shown in Figure 7. Several dispersion curves could be identified in Figure 7. In order to obtain the dispersion curves, the frequency and incident angle in Figure7 were converted into the frequency×thickness and phase velocity, and the result is shown in Figure 8. The peaks in frequency spectra were selected by the naked eyes. The subjective human error could be involved. However, the dispersion curves obtained from LLWs show very good agreement with the calculated one.

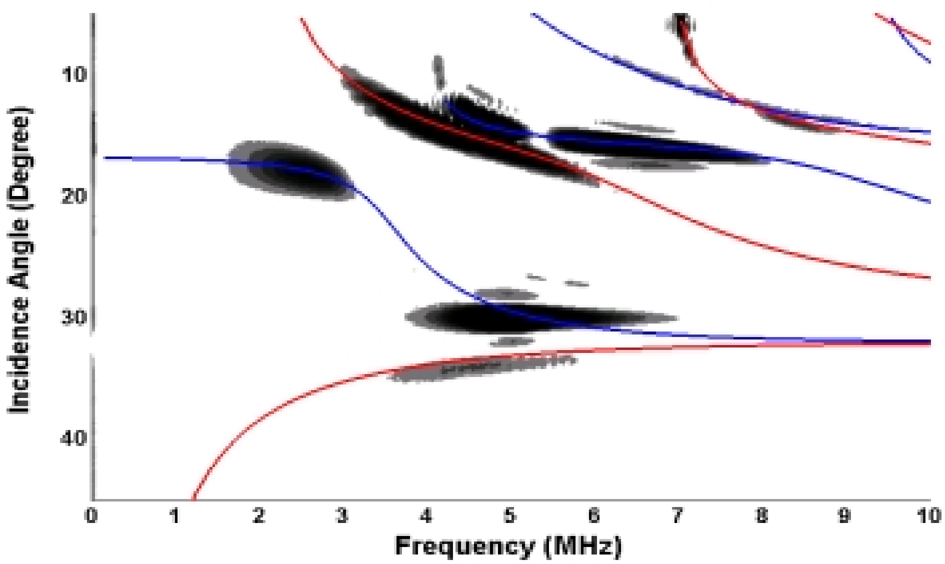

Figure 7. Gray scale representation of frequency spectra of leak Lamb waves by varing the incident angle.

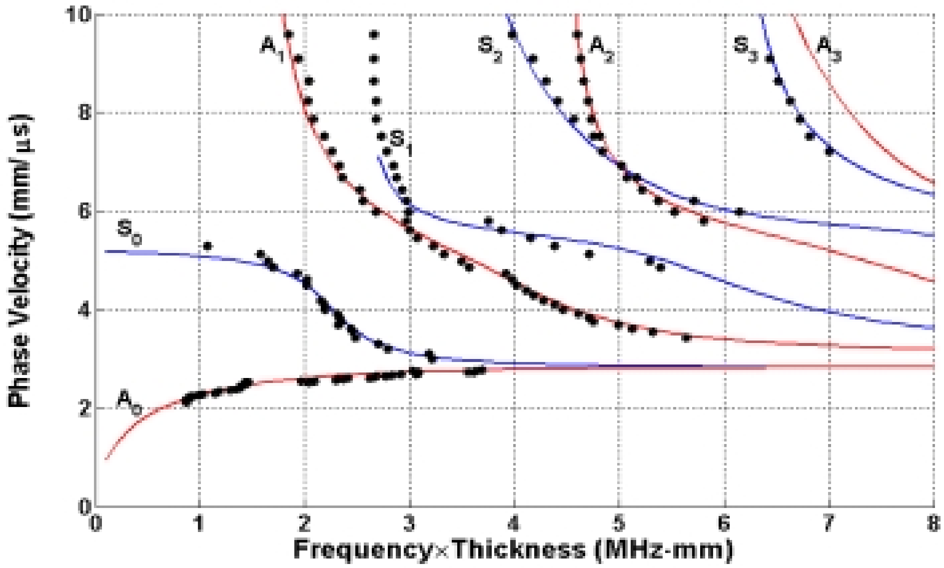

Figure 8. Phase velocity dispersion curves obtained by the leaky Lamb waves.

Determination of Group Velocities.

In order to determine the group velocities of Lamb waves, the incident position were moved in the linear direction of LLW propagation. As moving the incident position in the direction of increasing of beam distance, wave packets were moved as shown in Figure 9. The cross-correlation technique was adopted to measure the time delay. The front wave packet was identified as the S_1 mode of 6.53 MHz in the previous discussion. The measured time delay was 9.15 µs and the calculated group velocity was 4.37 mm/µs. Therefore, group velocity of the S_1 mode of 6.53 MHz was determined as 4.37 mm/µs. Similarly, the group velocity of the A_1 mode of 4.72 MHz was 3.36 mm/µs.

Figure 10 shows the LLW at the incident angle of 30.0°. As the incident position moves, there is little change in waveform. The group velocity of this mode turned out to be 3.02 mm/µs, which is similar to the velocity of Rayleigh surface wave. The typical group velocities at the different incident angles were observed as follows: At the incident angle of 13.0º, the group velocity of the S_1 mode of 4.50 MHz was 3.59 mm/µs. At the incident angle of 14.3º, those of the S_1 mode of 4.66 MHz and the A_1 mode of 4.18 MHz were 2.94 mm/µs and 2.62 mm/µs, respectively.

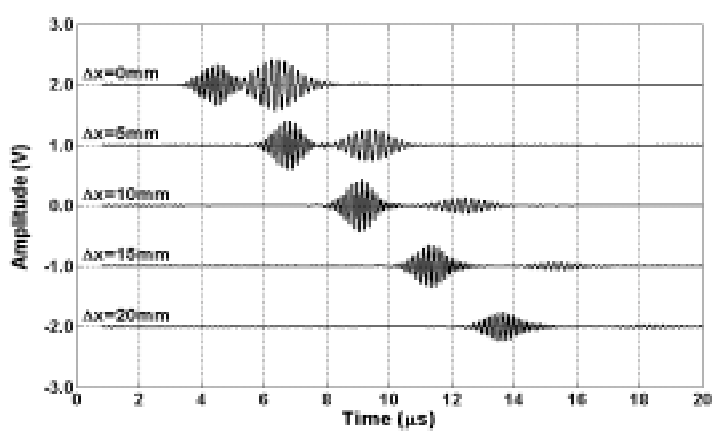

FIGURE 9. LLW for the moving incident position at the incident angle of 16.0º.

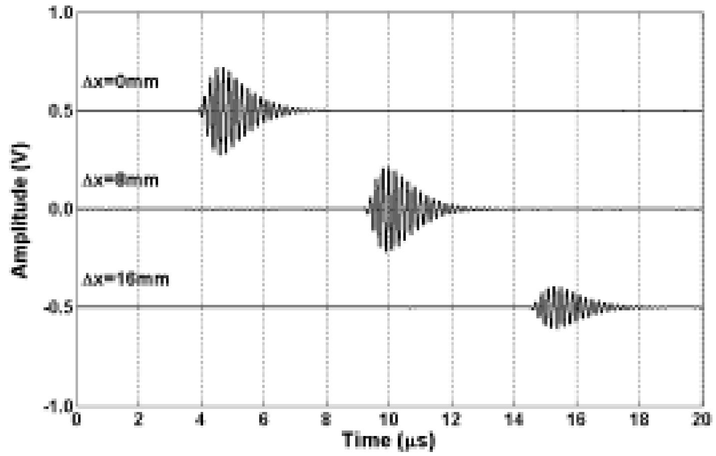

FIGURE 10. LLW for the moving incident position at the incident angle of 30.0º.

CONCLUSIONS

The profile of LLW has been measured using an home-made automated testing system. The phase velocity of Lamb wave was determined from the incident angle, and the frequency was determined from the spectrum of the backward radiation. Dispersion curves of phase velocities were determined from the relation between incident angles and frequency spectra of backward radiations. The group velocities were also determined from the time delay caused by moving the incident position.

ACKNOWLEDGEMENTS

Authors are grateful for the support in part provided by a grant from the Korea Science & Engineering Foundation (KOSEF) and Safety and Structural Integrity Research Center at the Sungkyunkwan University, South Korea.

REFERENCES

1. de Billy, M., Adler, L. and Quentin, G. *J. Acoust. Soc. Am.* **75**, 998 (1984).
2. Nagy, P. B., Jungman, A. and Adler, L. *Mater. Eval.* **46**, 97 (1988).
3. Chimenti, D. E. and Nayfeh, A. H. *J. Appl. Phys.* **58**, 4531 (1985).
4. Wilcox, P., Lowe, M. and Cawley, P. *NDT&E Int.* **34**, 1 (2001).
5. Pister, K. S. and Dong, S. B. *J. Eng. Mech. Div., Proc. Am. Soc. Civ. Eng.* **4**, 2194 (1959)
6. Lee, Y. -C. *Jpn. J. Appl. Phys.* **40**, 359 (2001).
7. Hayashi, Y., Ogawa, S., Cho., H. and Takemoto, M. *NDT&E Int.* **32**, 21 (1999).
8. Hernandez, C. M., Murray, T. W. and Krishnaswamy, S. *Appl. Phys. Lett.* **80**, 691 (2002)
9. Adler, L., de Billy, M., Quentin, G., Talmant, M. and Nagy, P. B. *J. Appl. Phys.* **68**, 6072 (1990).
10. Kown, S. D., Ko, R. T. and Adler, L. in *Review of Progress in QNDE*, Vol. 13, eds. D. O. Thompson and D. E. Chimenti, Plenum, New York, 1994, p. 1579.